ISSN No: -2456-2165 https://doi.org/10.38124/ijisrt/25jul1514

Assessing Rock Strength Degradation Under Temperature Variations using Brazilian Tensile Testing

Tolganay S. Jarassova[1*]; Renat K. Saudabayev[2]; Zarema M. Doyeva[3]; Nikita A. Pronin[4]

[1,2,3,4]Atyrau Branch LLP "KMG Engineering", 060097, Atyrau, Republic of Kazakhstan

Corresponding Author: Tolganay S. Jarassova[1*]

Publication Date: 2025/07/28

Abstract: Core samples are the most reliable source of geological data, yet their storage conditions are often neglected. Despite their scientific and economic value, cores are frequently kept in unheated shelters or outdoors, leading to property degradation and irreversible damage. Proper preservation requires controlled temperature, humidity, and environmental conditions—failure to maintain these results in both data and financial losses. This study examines how temperature fluctuations and humidity affect core integrity using the Brazilian test (uniaxial compression). Were analyzed 35 core samples from the H and BH fields (Precaspian Basin) under simulated seasonal cycles: heating (20°C, 60% humidity), freezing (−35°C), and dry heating (60°C). Results show progressive strength reduction, with samples deteriorating fastest under repeated freeze-thaw cycles. Data are presented via graphs and tables, demonstrating that improper storage significantly weakens core material over time. The findings highlight the need for climate-controlled storage to preserve core quality for future studies.

Keywords: *Core; Petrophysics; Brazilian Test; Uniaxial Compression; Temperature; Strength;* Destruction.

How to Cite: Tolganay S. Jarassova; Renat K. Saudabayev; Zarema M. Doyeva; Nikita A. Pronin (2025), Assessing Rock Strength Degradation Under Temperature Variations using Brazilian Tensile Testing. *International Journal of Innovative Science and Research Technology*, 10(7), 2196-2205. https://doi.org/10.38124/ijisrt/25jul1514

I. INTRODUCTION

Core material is a cylindrical sample extracted during drilling for further study. It serves as material for various laboratory analyses and is the most reliable source of geological information. Core data can provide insights into the geological structure of the subsurface, sedimentation conditions, the mineral composition of rocks, and the presence or absence of hydrocarbons. Often, this valuable information carrier is left in unsuitable storage conditions after studies, where the rock loses its properties, physical parameters, becomes friable, and becomes unsuitable for future repeated research (Figure 1, 2). Storing core material is one of the most critical criteria for preserving geological information. Unfortunately, necessary conditions are not always maintained, leading to rock destruction and data loss. Key parameters affecting rock structure changes [1, 3]:

Influence of Humidity. The most significant impact on core condition comes from daily and seasonal fluctuations in atmospheric humidity. Combined with temperature variations, these fluctuations activate geochemical processes that alter rock properties. The high heat capacity of rock-forming minerals leads to condensation of atmospheric moisture on them. The situation is far worse if the core is stored outdoors under atmospheric precipitation, even for a short time. The appearance of water droplets on certain rock types is highly undesirable. For example, in rocks containing halite, salt leaching occurs near the surface, leading to increased permeability and often making the core brittle and crumbly, resulting in its destruction. Clay minerals in rocks are also prone to hydration and swelling. Swelling is particularly relevant for friable cores and rocks with structural or film-pore clay content. Moistening such rocks leads to various consequences. Initially, the increase in volume of clay minerals narrows pore channels and worBHs filtration-capacity properties (FCP). Excessive swelling further causes rock destruction.

Influence of Temperature Fluctuations. Temperature fluctuations also significantly affect core condition. Heating and cooling of the core throughout the year cause uneven expansion and contraction of minerals in the rock, typically manifesting as microcracks and potential rock layering. However, this effect is magnified if the core is poorly dried and stored in unsuitable conditions. Slow freezing of moisture

ISSN No: -2456-2165 https://doi.org/10.38124/ijisrt/25jul1514

inside the core leads to the formation of large ice crystals, causing cracks and changes in pore space structure (similar to frost weathering). Subsequent temperature increases during seasonal changes thaw the ice-filled cracks, leaving them open and unfilled, further contributing to rock friability. Table 1 below demonstrates changes in temperature and humidity over a year, illustrating their impact on core destruction and the need for proper storage conditions [1, 2].

Fig 1 The Core is Stored Under a Canopy Outside, Subject to Changes in Temperature and Humidity.

Fig 2 A Core Stored in a Core Storage Facility Under Proper Storage Conditions.

Table 1 Temperature Change Throughout the Year

Indicator	Jan.	Feb.	Mar.	Apr.	May	June	July	Aug.	Sep.	Oct.	Nov.	Dec.	Year
Absolute maximum, °C	10,5	15,0	26,3	32,5	38,9	42,8	42,7	44,6	40,1	29,6	20,0	11,8	44,6
Average maximum, °C	−2,8	−1,8	5,8	17,2	24,5	30,8	33,4	31,6	24,6	15,3	5,1	−1,1	15,2
Average temperature, °C	−6,4	−5,6	1,9	11,6	19,4	25,1	27,4	25,6	18,4	10,2	1,5	−4,2	10,4
Average minimum, °C	−9,4	−9,9	−3,1	6,1	12,8	18,4	20,5	18,5	12,3	5,0	−1,7	−7	5,2
Absolute minimum, °C	−37,9	−37,4	−32,3	−12,3	−2,3	2,3	8,1	4,8	−5,7	−15,7	−29,8	−35,8	−37,9
Precipitation norm, mm	16	12	16	17	28	17	12	10	9	18	16	16	186

Alongside these properties, the rock also loses strength due to temperature influences. The tensile strength of rocks is a key parameter for determining the load-bearing capacity of elements in the Earth's subsurface for many geological processes [1]. To assess the degree of rock destruction, this study subjected samples to temperature variations and then to the Brazilian test.

The Brazilian test is the simplest indirect method for determining the tensile strength of rocks. In this test, a cylindrical sample, typically with a thickness equal to its radius, is diametrically compressed until failure. Since its inception, the test has undergone many modifications, one of which was applied in this study of rock destruction under temperature variations during uniaxial compression. In this study, were recreated models of temperature changes and by subjecting samples to these fluctuations, demonstrated the degree of change in rock strength using the method - "Brazilian test" [4-6].

II. RESEARCH METHODOLOGY

To determine the strength properties of rocks using the Brazilian test, cylindrical core samples of terrigenous and carbonate rocks—sandstone, clay, siltstone, and limestone—were used. These were extracted from wells No. 708 at the H

ISSN No: -2456-2165 https://doi.org/10.38124/ijisrt/25jul1514

field and No. 33 at the BH field. Drilling cylindrical rock samples was performed using an SVOK-100 drilling rig with a diamond bit and cooling fluid. After drilling, the ends of each sample were trimmed using an SOOK-3 machine to obtain averaged results. A total of 35 samples were drilled with horizontal bedding orientation. Each sample under study was numbered according to the sampling interval, trip and well (Figure 4). Table 2 below presents the characteristics of the studied samples.

Fig 3 Appearance of Cylindrical Core Samples from Well # 708 H Field and Well # 33 BH Field

Table 2 Dimensional Values of the Studied Samples

Initial length of the sample after drilling, mm	Standard length of sample without endnotes, mm	Sample diameter, mm
100	20	38

For further Brazilian testing and determination of various properties, samples must be clean and free of saturating fluids. Thus, after shaping and labeling, samples were sent for extraction. Cleaning was performed in a Soxhlet apparatus using organic solvents (alcohol-benzene mixture) [7]. After complete cleaning, samples were dried in an oven (DKN 600) at 60°C until constant weight. After obtaining basic volume and weight parameters, samples were placed in a glass desiccator to minimize atmospheric moisture adsorption and forwarded for standard analysis (porosity and gas permeability determination). For measuring capacitive-filtration parameters, accurate dimensions of cylindrical samples are crucial. An "Abacus" computerized station was used for automated data input on sample weight and dimensions [8]. Weighing was performed on analytical balances with 0.001 g precision, and average sample dimensions were measured using a digital caliper.

Measurement of porosity, bulk and mineralogical density of core samples. A calibrated helium porosimeter (ULTRA-PORE 300) operating on Boyle's law (1) was used to measure grain volume.

$$P_1 \cdot V_1 = P_2 \cdot V_2 \quad (1)$$

A calibrated helium porosimeter (ULTRA-PORE 300) operating on Boyle's law (1) was used to measure grain volume:

$$P_1 \cdot V_{Ref} = P_2 \cdot \left(V_{Ref} + V_{Matrix} - V_{grain}\right) \quad (2)$$

Where:

P_1 - pressure in the comparison chamber;
V_{Ref} - volume of the comparison chamber, cm3;
P_2 - pressure after helium diffusion in the core glass;
V_{Matrix} - volume of the core cup, cm3;
V_{grain} - volume of sample grain, cm3.

Next, the porosity (3), bulk density (4) and mineralogical density (6) of the rock sample were calculated using the following formulas [8]:

$$\varphi = \frac{(L \cdot \pi \cdot \frac{D^2}{4}) - V_{Зерна}}{(L \cdot \pi \cdot \frac{D^2}{4})} \cdot 100 \quad (3)$$

$$\rho = \frac{m}{(L \cdot \pi \cdot \frac{D^2}{4})} \quad (4)$$

ISSN No: -2456-2165 https://doi.org/10.38124/ijisrt/25jul1514

$$\rho_{miner} = \frac{m}{V_{grain}} \quad (5)$$

Where:

φ– sample porosity, %;
L– sample length, cm;
D– sample diameter, cm;
ρ – bulk density of the sample, g/cm3;
$\rho_{минер}$– mineralogical density of the sample (grain density), g/cm3;
$m_{обр}$– dry weight of the sample, g.

It should be noted that a certain porosity is implied as open porosity and, accordingly, the mineralogical density of the rock has an apparent mineralogical density if closed porosity is preBHt in the sample under study.

Measurement of absolute permeability of samples. A calibrated helium porosimeter (ULTRA-PORE 300) operating on Boyle's law (1) was used to measure grain volume.

The basic Darcy equation for calculating gas permeability is as follows [9]:

$$K_g = \frac{2000 \cdot P_1 \cdot \mu \cdot Q_1 \cdot L}{(P_1^2 - P_2^2) \cdot A} \quad (6)$$

Where:

Kg– gas permeability, mD;
μ– gas viscosity, cP;
Q_1-gas flow rate, cm3/sec;
P_1–input pressure, atm;
P_2–descending pressure, atm;
A– cross-sectional area of the sample perpendicularly, cm2;
L– sample length, cm.

III. EXPERIMENTAL RESULTS

The results of standard core analysis such as lithology, porosity, mineralogical density, and permeability were presented in the Table 3. Fine-medium grained sandstones (samples 1-6) exhibit higher porosity (17.2-29.5%) and permeability (9.38-969.90 mD), while silty sandstones (samples 7-23) show moderate porosity (14.5-19.5%) and variable permeability (0.42-15.40 mD). Clay-rich samples (24-26) and limestones (32-35) demonstrate lower porosity (6.9-19.0%) and significantly reduced permeability (0.07-2.41 mD), with calcareous samples showing the lowest values. Notably, mineralogical density remains relatively consistent (2.69-2.72 g/cm³) across all lithologies, suggesting similar mineral compositions despite varying textures. The data reveals an inverse relationship between depth and permeability in sandstone samples, with shallower samples (1222-1778m) showing higher permeability than deeper ones (1782-1791m), likely due to compaction effects.

Table 1 Summary Table of Core Samples After Standard Analyses

Item No.	Depth of selection sample, m	Well	Field	Porosity, %	Mineralogical rock density, g/cm3	Permeability by gas, mD	Brief lithology
1	1222,18	33	BH	29.5	2.69	969.90	Fine-medium grained sandstone
2	1226.6	33	BH	28.3	2.71	569.30	Fine-medium grained sandstone
3	1766.35	33	BH	17.7	2.72	51.80	Fine-medium grained sandstone
4	1768.8	33	BH	17.9	2.69	14.10	Fine-grained sandstone
5	1769,1	33	BH	17.2	2.70	9.38	Fine-grained sandstone
6	1769.4	33	BH	19.3	2.70	22.80	Fine-grained sandstone
7	1773,5	33	BH	17.5	2.69	7.18	Silty sandstone
8	1775.3	33	BH	17.5	2.69	11:30	Silty sandstone
9	1776	33	BH	19.5	2.71	15.40	Silty sandstone
10	1778.3	33	BH	16.3	2.69	6.37	Silty sandstone
11	1778,55	33	BH	18.2	2.69	7.97	Silty sandstone
12	1782.75	33	BH	15.4	2.70	0.68	Fine-grained sandstone
13	1782.95	33	BH	15.1	2.71	0.28	Fine-grained sandstone
14	1784.5	33	BH	16.5	2.70	1.60	Fine-grained sandstone
15	1785.1	33	BH	14.5	2.70	0.42	Silty sandstone
16	1785.6	33	BH	14.7	2.71	0.88	Silty sandstone
17	1787,1	33	BH	17.0	2.70	8.95	Silty sandstone
18	1787.3	33	BH	16.9	2.69	15:30	Silty sandstone
19	1787,5	33	BH	15.8	2.69	5.90	Silty sandstone
20	1790,15	33	BH	16.4	2.70	3.49	Fine-grained sandstone

ISSN No: -2456-2165 https://doi.org/10.38124/ijisrt/25jul1514

21	1790.4	33	BH	18.2	2.70	10.80	Silty sandstone
22	1791,1	33	BH	16.8	2.69	8.92	Silty sandstone
23	1791.85	33	BH	16.5	2.69	4.74	Silty sandstone
24	1844.93	708	H	17.3	2.69	0.62	Silty clay with admixture
25	1862,15	708	H	19.0	2.69	1.96	Lime clay
26	1867,77	708	H	18.0	2.70	2.41	Alternation of clay and sandstone
27	1868.27	708	H	15.0	2.71	0.31	Fine-grained sandstone
28	1869.87	708	H	16.3	2.70	2.36	Fine-grained sandstone
29	1871,87	708	H	15.9	2.70	0.27	Fine-grained sandstone
30	1879,68	708	H	17.8	2.69	0.88	Fine-grained, calcareous sandstone
31	1888,55	708	H	12.6	2.72	0.70	Calcareous siltstone
32	1892.2	708	H	6.9	2.71	0.07	Limestone
33	1909,94	708	H	17.6	2.70	0.44	Limestone
34	1919,84	708	H	17.8	2.71	13.60	Fine-grained sandstone
35	1928,72	708	H	12.5	2.72	1.15	Limestone

Creating a climate change model. Cylindrical samples were subjected to temperature variations in 8 stages.

➢ *Stage 1:*

Measuring the maximum strength of samples not subjected to temperature variations under uniaxial compression using two polished plates. After obtaining initial pressure data, samples were subjected to simulated seasonal climate changes:

- Heating to 20°C at 60% humidity — Autumn climate
- Freezing at -35°C — Winter climate
- Thawing at room temperature (+17-22°C) — Spring climate
- Heating to 60°C without humidity — Summer climate

Heating and freezing cycles were repeated until all samples were destroyed. Each stage represented one year of core storage. Table 4 below shows the number of samples destroyed at each stage. In the initial stage with no thermal stress (Stage 1), all 35 samples remained intact, establishing a baseline. The subsequent stages (2-6) implementing gradual but significant destruction, with Stages 2, 3, 4, 5, and 6 destroying 6, 4, 5, 8, and 5 samples respectively - showing that cyclic freezing-thawing is particularly damaging when combined with humidity variations. The introduction of summer conditions (60°C dry heating) in Stages 7-8 resulted in the destruction of 4 and 3 additional samples, suggesting that extreme dry heat following freeze-thaw cycles further compromises rock stability. The complete destruction of all 35 samples after eight annual cycles (equivalent to eight years of improper storage) demonstrates that improper environmental conditions lead to progressive, irreversible damage to core samples.

Table 2 Summary Table by Parameters

Stage #	Heating, °C	Humidity during heating, %	Heating time with humidity, hours	Freezing °C	Freezing time, hours	Defrosting, °C	Heating, without humidity*, °C	Heating time without humidity, hours	Number of samples destroyed
Stage 1	-	-	-	-	-	-	-	-	0
Stage 2	+20	60	5	-35	12	+17/22	-	-	6
Stage 3	+20	60	5	-35	12	+17/22	-	-	4
Stage 4	+20	60	5	-35	12	+17/22	-	-	5
Stage 5	+20	60	5	-35	12	+17/22	-	-	8
Stage 6	+20	60	5	-35	12	+17/22	-	-	5
Stage 7	+20	60	5	-35	12	+17/22	60	12	4
Stage 8	+20	60	5	-35	12	+17/22	60	12	3
Climate	Autumn			Winter		Spring	Summer		**35**

After each stage, samples were immediately subjected to the Brazilian test. Prepared rock samples were placed between specially equipped polished plates, with the sample axis parallel to the press planes, and subjected to gradually increasing pressure until failure. The maximum pressure reading was recorded as the destructive load. Figure 5 shows the stages of sample destruction. Samples that did not fail were returned to the oven, and the process was repeated seven times. This demonstrates that after more than five years of

ISSN No: -2456-2165 https://doi.org/10.38124/ijisrt/25jul1514

improper storage, core begins to degrade and lose its properties.

During the study, it was noted that no sample replicated initial data under repeated loading. One group of samples became friable, while another became stronger due to changes in mineral composition and grain deformation. All obtained data are fully presented in Table 5. For comprehensive results, scatter histograms were builded (Figures 5-11). Applied pressure data for each sample group were compared with initial Group 1 results.

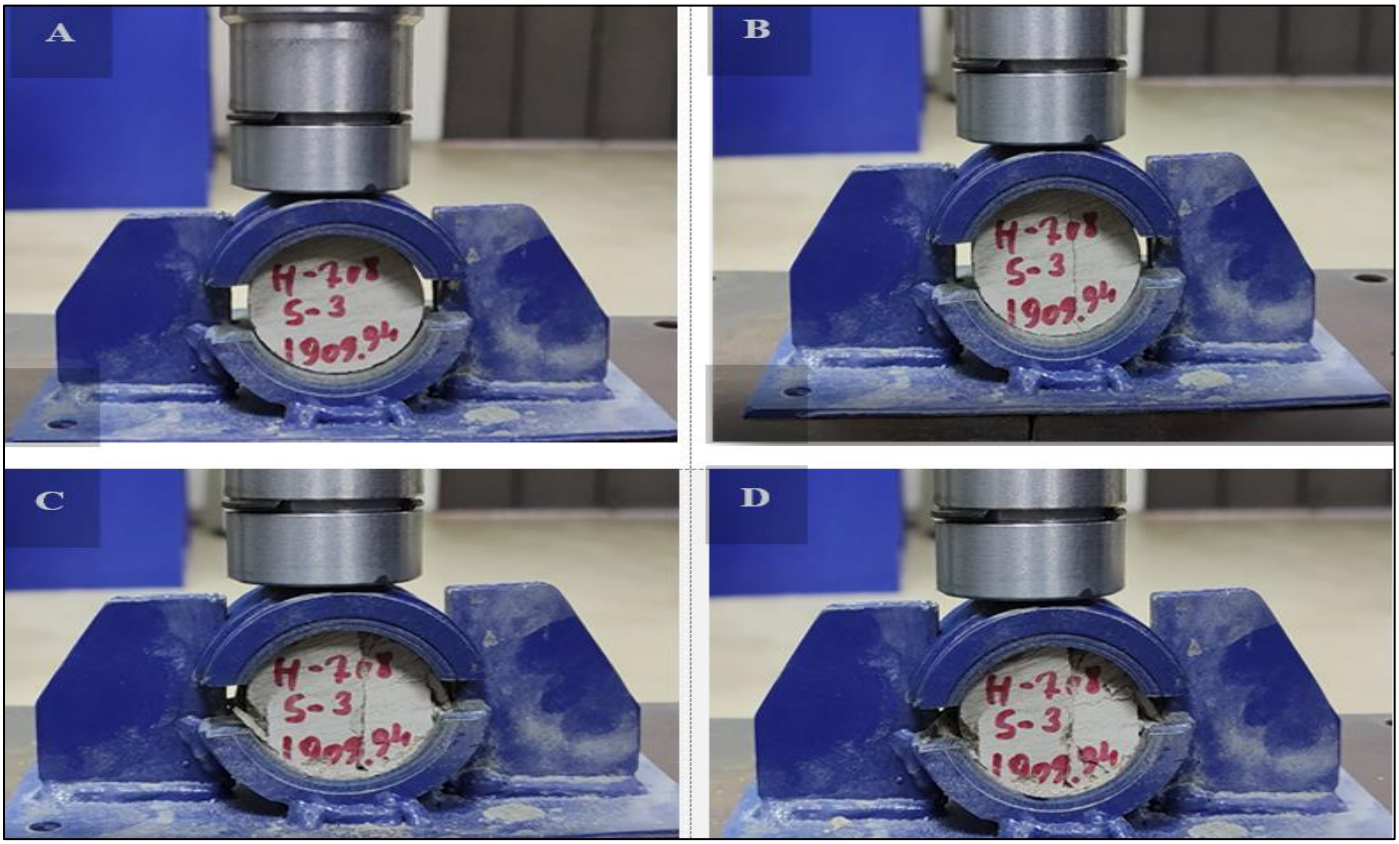

Fig 4 The Process of Experimental Work on Increasing the Load on the Sample

Table 5 Summary Table with the Obtained Results on the Pressure Change After Each Experiment of the Brazilian Test

#	Sampling depth, m	Well	Field	Porosity, %	Bulk density rocks, g/cm3	Mineralogical density rocks, g/cm3	Gas permeability, mD	Lithology	Stages with the number of destroyed samples and the applied pressure.							
									1. stage, MPa	2. stage, MPa	3. stage, MPa	4. stage, MPa	5. stage, MPa	6. stage, MPa	7. stage, MPa	8. stage, MPa
1	1222, 18	33	BH	29.5	1.90	2.69	969.90	Fine-medium grained sandstone	2.83		3.34					
2	1226. 6	33	BH	28.3	1.94	2.71	569.30	Fine-medium grained sandstone	3.11	3.02						
3	1766. 35	33	BH	17.7	2.24	2.72	51.80	Fine-medium grained sandstone	3.35			8.11				
4	1768. 8	33	BH	17.9	2.21	2.69	14.10	Fine-grained sandstone	13.15	7.63						
5	1769, 1	33	BH	17.2	2.24	2.70	9.38	Fine-grained sandstone	12.15			10.73				
6	1769. 4	33	BH	19.3	2.18	2.70	22.80	Fine-grained sandstone	10.76	7.72						

ISSN No: -2456-2165 https://doi.org/10.38124/ijisrt/25jul1514

7	1773,5	33	BH	17.5	2.22	2.69	7.18	Silty sandstone	13.75				11.3			
8	1775.3	33	BH	17.5	2.22	2.69	11:30	Silty sandstone	13.28				7.63			
9	1776	33	BH	19.5	2.18	2.71	15.40	Silty sandstone	8.59					8.14		
10	1778.3	33	BH	16.3	2.25	2.69	6.37	Silty sandstone	16.66				11.27			
11	1778,55	33	BH	18.2	2.20	2.69	7.97	Silty sandstone	14.71				7.5			
12	1782.75	33	BH	15.4	2.28	2.70	0.68	Fine-grained sandstone	15.06							15.25
13	1782.95	33	BH	15.1	2.30	2.71	0.28	Fine-grained sandstone	14.06				11.87			
14	1784.5	33	BH	16.5	2.26	2.70	1.60	Fine-grained sandstone	12.36					7.82		
15	1785.1	33	BH	14.5	2.31	2.70	0.42	Silty sandstone	15.53		8.18					
16	1785.6	33	BH	14.7	2.31	2.71	0.88	Silty sandstone	13.64							13.59
17	1787,1	33	BH	17.0	2.24	2.70	8.95	Silty sandstone	9.09				11.9			
18	1787.3	33	BH	16.9	2.24	2.69	15:30	Silty sandstone	15.34						16.48	
19	1787,5	33	BH	15.8	2.26	2.69	5.90	Silty sandstone	11.6			11.18				
20	1790,15	33	BH	16.4	2.26	2.70	3.49	Fine-grained sandstone	12.35					7.63		
21	1790.4	33	BH	18.2	2.21	2.70	10.8	Silty sandstone	10.84						10.4	
22	1791,1	33	BH	16.8	2.24	2.69	8.92	Silty sandstone	14.17			9.42				
23	1791.85	33	BH	16.5	2.25	2.69	4.74	Silty sandstone	11.45		11.23					
24	1844.93	708	H	17.3	2.22	2.69	0.62	Clay with silt impurity	12.11						18.25	
25	1862,15	708	H	19.0	2.18	2.69	1.96	Lime clay	6.09							10.54
26	1867,77	708	H	18.0	2.22	2.70	2.41	Alternation of clay and sandstone	5.43		4.32					
27	1868.27	708	H	15.0	2.30	2.71	0.31	Fine-grained sandstone	8.61			5.51				
28	1869.87	708	H	16.3	2.26	2.70	2.36	Fine-grained sandstone	5.33				6.63			
29	1871,87	708	H	15.9	2.27	2.70	0.27	Fine-grained sandstone	7.16				5.25			
30	1879,68	708	H	17.8	2.21	2.69	0.88	Fine-grained, calcareous sandstone	13.48						8.85	
31	1888,55	708	H	12.6	2.37	2.72	0.70	Calcareous siltstone	7.11					7.48		
32	1892.2	708	H	6.9	2.52	2.71	0.07	Limestone	6.63	11.21						
33	1909,94	708	H	17.6	2.22	2.70	0.44	Limestone	13.96	11.88						
34	1919,84	708	H	17.8	2.23	2.71	13.6	Fine-grained sandstone	13.67	13.24						
35	1928,72	708	H	12.5	2.38	2.72	1.15	Limestone	15.91					18.96		

ISSN No: -2456-2165 https://doi.org/10.38124/ijisrt/25jul1514

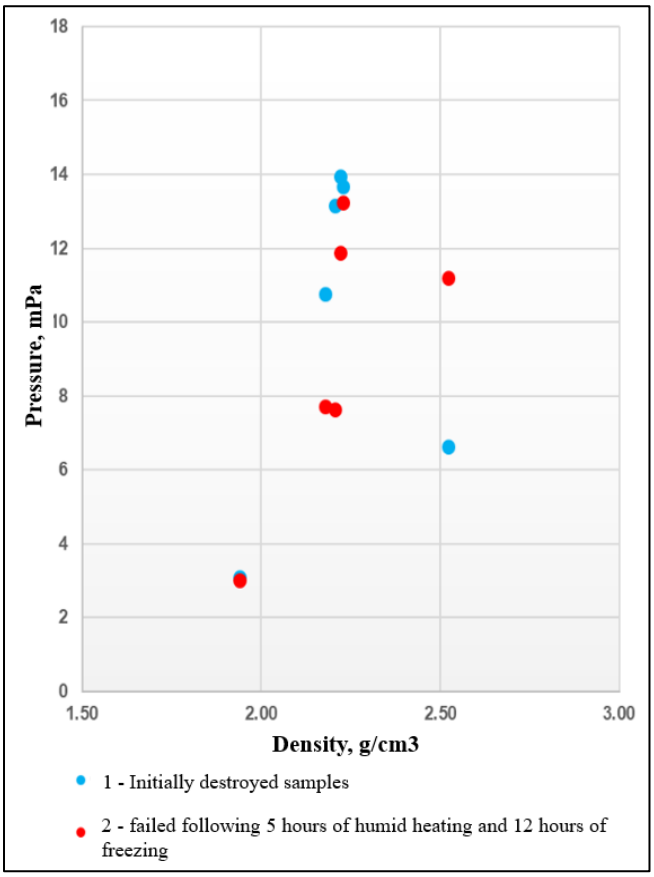

Fig 5 Pressure vs Density of Samples Between the 1st Stage and the 2nd Stage

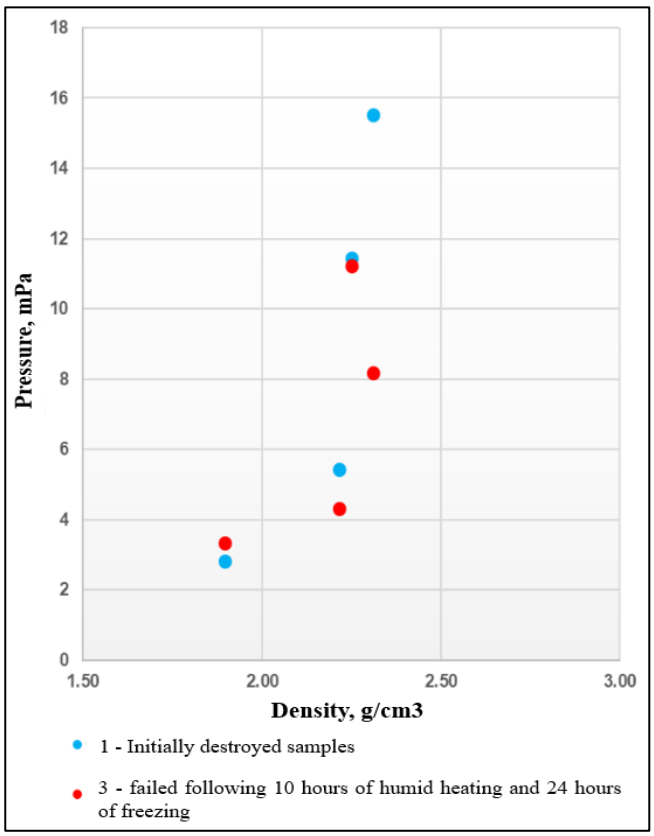

Fig 6 Pressure vs Density of Samples Between the 1st Stage and the 3rd Stage

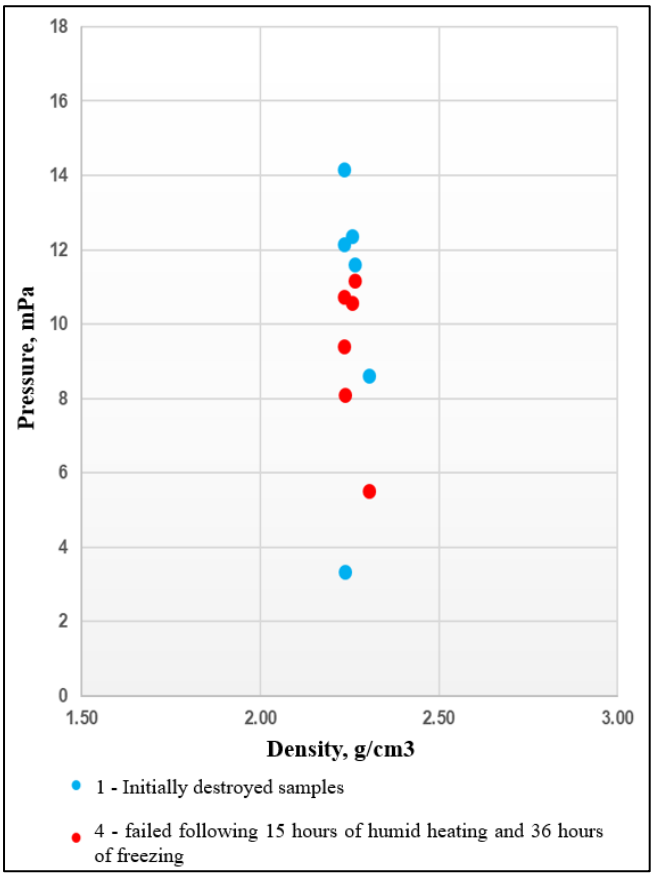

Fig 7 Pressure vs Density of Samples Between the 1st Stage and the 4th Stage

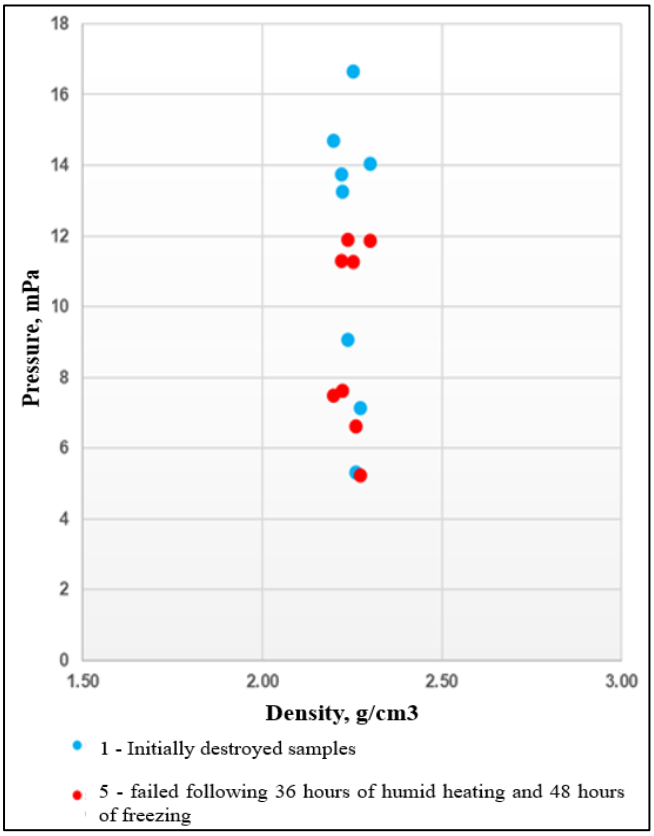

Fig 8 Pressure vs Density of Samples Between the 1st Stage and the 5th Stage

ISSN No: -2456-2165 https://doi.org/10.38124/ijisrt/25jul1514

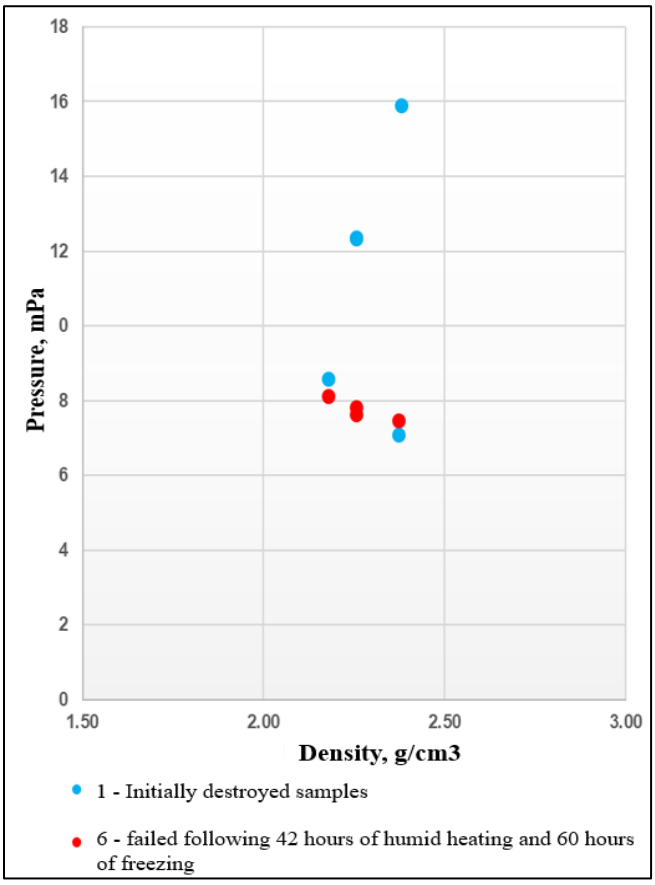

Fig 9 Pressure vs Density of Samples Between the 1st Stage and the 6th Stage

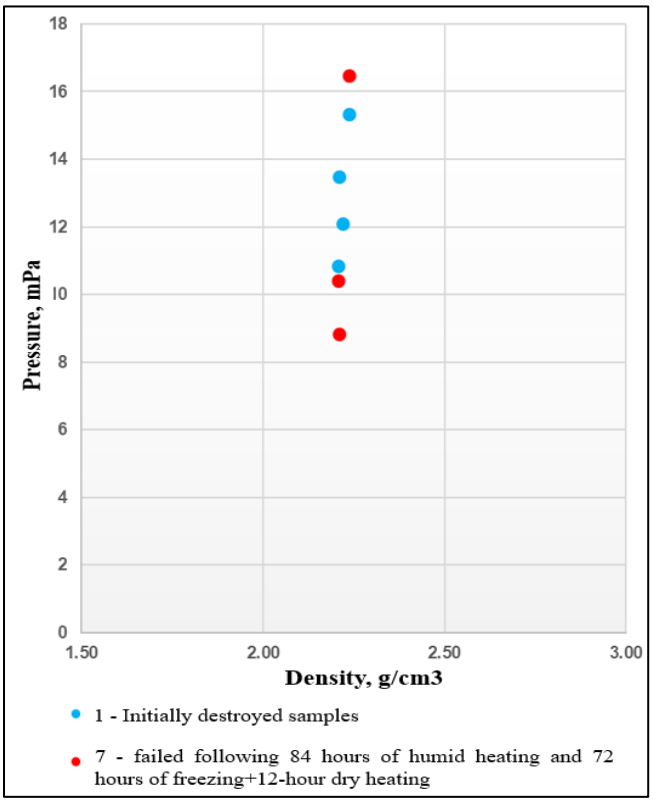

Fig 10 Pressure vs Density of Samples Between the 1st Stage and the 7th Stage

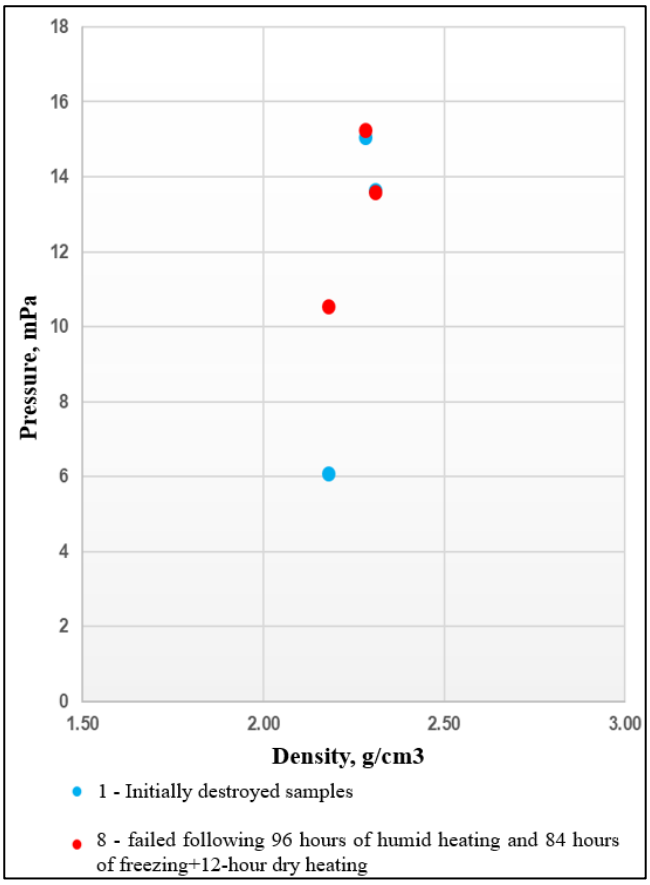

Fig 11 Pressure vs Density of Samples Between the 1st Stage and the 8th Stage

IV. CONCLUSIONS

This study with the creation of climate change models was conducted to obtain information on the degree of change in the strength of core material under uniaxial compression by grinding plates. It was proven that if proper storage conditions are not maintained, the core material loses its original properties in the form of density, strength and even mineral composition. These changes lead to the fact that the rock becomes unsuitable for repeated studies after a certain amount of time. The results of experimental studies demonstrated the effect of alternating temperature effects on the destruction of core material samples. The work provides a solution to the problem of establishing patterns of change in rock destruction under alternating temperature effects. Changes in rock temperature can have a very serious effect on the rock. Its increase can lead to a decrease in the strength limits of the sample under study, and at certain temperature limits, changes can occur in the mineralogical structure of the rock. Radical changes are also observed within the strength ratio and elastic properties. Mechanical properties of rocks also change significantly when they are frozen. The main results, conclusions and patterns of the study conducted using the Brazilian test are:

- The application of the method for determining the energy intensity of rock destruction allows us to estimate the specific energy intensity of rock destruction under alternating temperature effects.

ISSN No: -2456-2165 https://doi.org/10.38124/ijisrt/25jul1514

- The degree of influence of temperature on the destruction of a cylindrical core sample depends on its density and lithological structure.

- It has been established that the impact on rocks during 8 different heating-freezing-thawing cycles leads to a change in the physical parameters of the rock, a decrease in its density and a change in the mineral composition.

- The decrease in density and specific energy capacity of destroyed rocks is explained by the fact that when the temperature decreases, internal stress arises in the material, caused primarily by a change in the aggregate state of water (with humidity), as well as by differences in elastic properties and thermal expansion coefficients of individual grains of rock.

- The obtained and demonstrated research results in this article on the influence of alternating temperature effects on the process of rock destruction, measured by the Brazilian test, can serve as a recommendation for carrying out measures to ensure the correct storage of core material in a core storage facility for its long-term preservation of its original appearance and properties.

REFERENCES

[1]. R. Ulusay. ISRM Suggested Methods. Rock Characterization Testing and Monitoring, Suggested methods for determining the tensile strength of rock materials. (n.d.). Oxford: Pergamon Press, 2015.
[2]. Ye Jianhong, F. J. International Journal of Rock Mechanics & Mining Sciences. 2009.
[3]. Goncharov, S. A. Physical and technical foundations of resource conservation during rock destruction. Moscow: MGGU. 2009.
[4]. Luca Pelà, Konstantina Kasioumi, Pere Roca. Experimental evaluation of the shear strength of aerial lime mortar brickwork by standard tests on triplets and non-standard tests on core samples. Engineering Structures. 2017. Available from https://www.researchgate.net/publication/312218965.
[5]. Timothy R.M. Packulak, Jennifer J. Day, Mark R. McDonald, Anya C. Jacksteit, and Mark S. Diederichs. Measurement of true tensile strength from Brazilian tensile strength laboratory tests. Canadian Science Publishing, 62. 2025. dx.doi.org/10.1139/cgj-2023-0204
[6]. AlAwad, M.N.J. Modification of the Brazilian indirect tensile strength formula for better estimation of the tensile strength of rock and rock-like geomaterials. Journal of King Saud University. Engineering Sciences, 2020. doi: 10.1016/j.jksues.2020.08.003.
[7]. Eliseev V.V. Mekhanika deformiruemogo tverdogo tela [Mechanics of a deformable solid], St. Petersburg, Polytechnic University Publish., 2006, 231 p. (in Russ.)
[8]. Kotyakhov, F. I. Fundamentals of petroleum reservoir physics. Nedra. 1986 (in Russ.)
[9]. Darcy Henry. Les fontaines publiques de la ville de Dijon: exposition et application des principes à suivre et des formules à employer dans les questions de distribution d'eau. — Paris: V. Dalmont, 1856.